# Supplementary Information

# Ligand-protected and lowered-temperature hydrothermal synthesis of platinum encapsulated in TON zeolite for shape-selective hydrogenation of furfural to furfuryl alcohol

Xuelin Wang,[a,b] Congxin Wang,*[a] Wentao Bi,[a,b] Wei Qu[a] and Zhijian Tian*[a]

[a] Dalian National Laboratory for Clean Energy, State Key Laboratory of Catalysis, Dalian Institute of Chemical Physics, Chinese Academy of Sciences, 457 Zhongshan Road, Dalian 116023, China

[b] University of Chinese Academy of Sciences, Beijing 100049, China

*Corresponding author. E-mail: C. Wang (*): wangcx@dicp.ac.cn, Z. Tian (*): tianz@dicp.ac.cn

**Table of Contents**

**Fig. S4.** (a) XRD patterns of the samples synthesized with the molar composition of 100 $SiO_2$: 37.5 HDA: 5 $K_2O$: 3800 $H_2O$: 8.86 $NH_2CH_2CH_2NH_2$: 0.185 $[Pt(en)_2]Cl_2$ at 140 °C for different time. (b) The corresponding crystallization curves of the samples. The relative crystallinity was calculated based on the XRD patterns in (a) by the ratio of the sum of the XRD peak aera at 2θ=8.2°, 10.2°, 12.8°, 16.4°, 19.5°, 20.4°, 24.3°, 24.7°, 25.8°, 35.7° of the sample synthesized for different time to that of the well-crystallized sample for 24 h.

**Table S2.** Chemical composition (wt.%) of the $Pt_{0.6}$@ZSM-22-H and ZSM-22-H determined by XRF.

**Table S3.** EXAFS data fitting results of Pt of $Pt_{0.6}$@ZSM-22-H and $Pt_{0.6}$/ZSM-22-H.

**Table S4.** Comparison of catalytic performances of various Pt-based and zeolite-based catalysts for the conversion of furfural (FFL) to furfuryl alcohol (FOL) in the liquid phase.

**Table S5.** The absorption band assignment of IR spectrum of liquid-phase furfural, gas-phase furfural and adsorbed furfural.

**Table S1.** Pt loading, Pt surface site concentration and average particle size.

| Sample | Pt loading[a] (wt.%) | $C_{H_2}$[b] (μmol/g) | $d_{TEM}$[c] (nm) |
|---|---|---|---|
| $Pt_{0.6}$@ZSM-22-H-C | 0.62 | 10.0 | 3.6 |
| $Pt_{0.6}$@ZSM-22-C-H | 0.62 | 6.8 | 8.9 |
| $Pt_{0.6}$/ZSM-22-H | 0.33 | 10.5 | 2.5 |
| $Pt_{0.6}$/ZSM-22-H-C | 0.33 | 6.1 | 9.9 |

[a] By ICP-OES. [b] The concentration of Pt surface sites. [c] The average particle size of Pt determined by TEM.

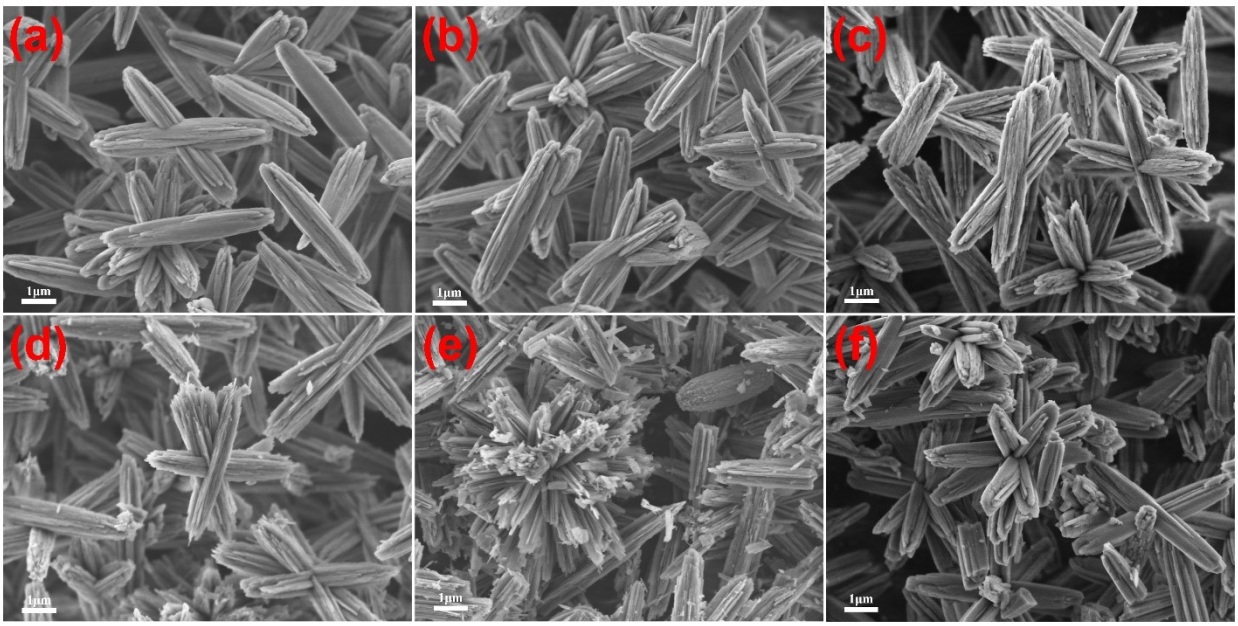


**Fig. S1.** SEM images of (a) $Pt_{0.2}$@ZSM-22-H, (b) $Pt_{0.4}$@ZSM-22-H, (c) $Pt_{0.6}$@ZSM-22-H, (d) $Pt_{0.8}$@ZSM-22-H, (e) $Pt_{1.0}$@ZSM-22-H, (f) ZSM-22-H.

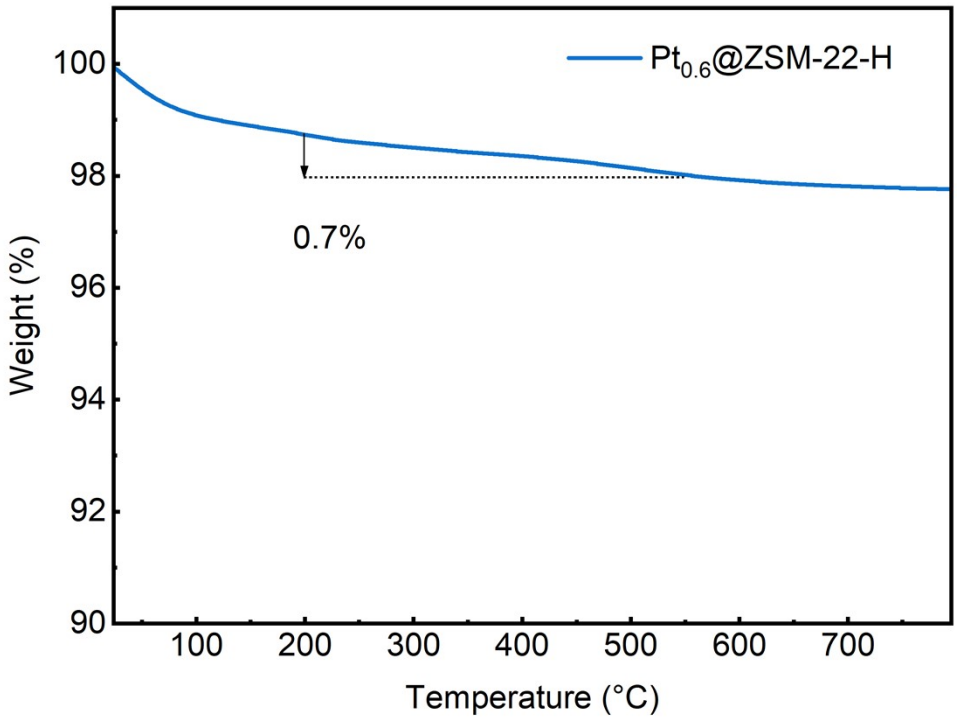


**Fig. S2.** TG curve of $Pt_{0.6}$@ZSM-22-H.

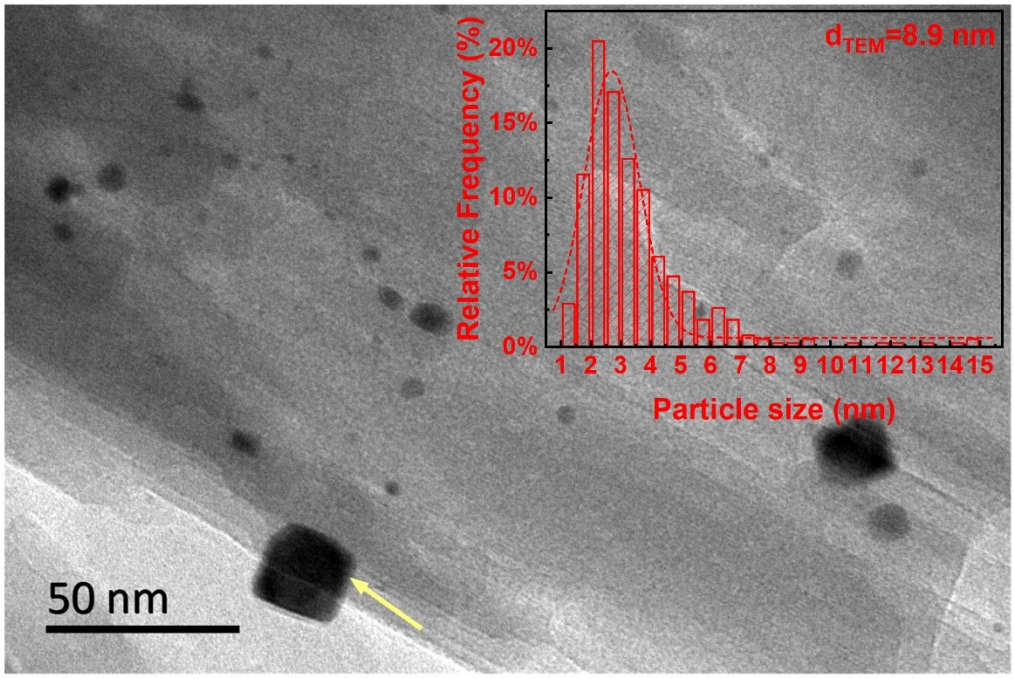


**Fig. S3.** TEM image and Pt particle size distribution of $Pt_{0.6}$@ZSM-22-C-H. The sample was reduced at 400 °C before the image was collected.

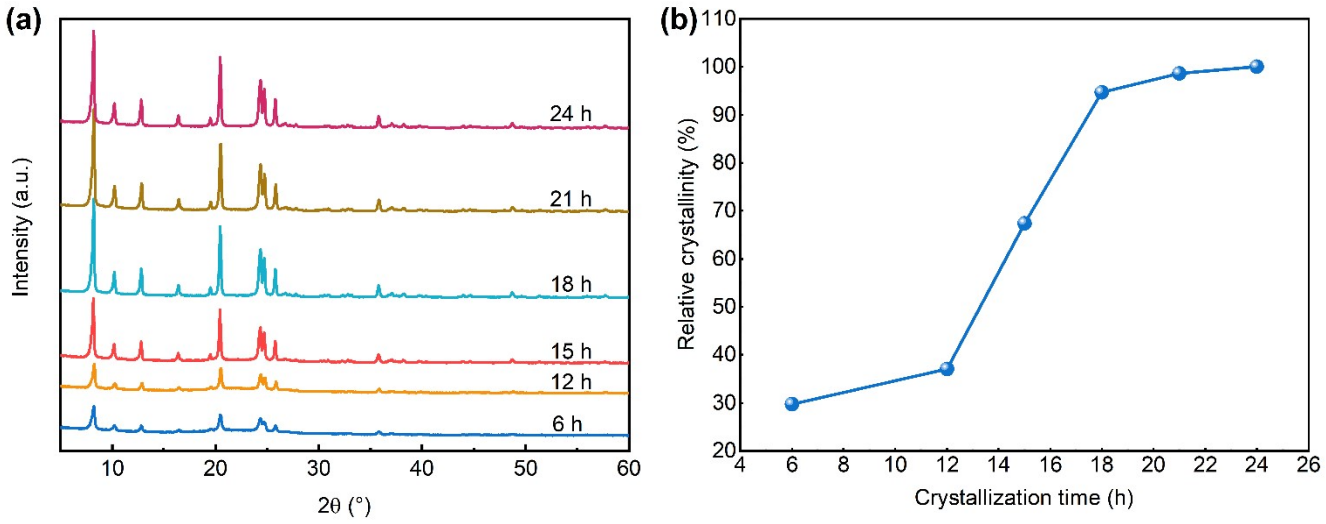


**Fig. S4.** (a) XRD patterns of the samples synthesized with the molar composition of 100 $SiO_2$: 37.5 HDA: 5 $K_2O$: 3800 $H_2O$: 8.86 $NH_2CH_2CH_2NH_2$: 0.185 $[Pt(en)_2]Cl_2$ at 140 °C for different time. (b) The corresponding crystallization curves of the samples. The relative crystallinity was calculated based on the XRD patterns in (a) by the ratio of the sum of the XRD peak aera at 2θ=8.2°, 10.2°, 12.8°, 16.4°, 19.5°, 20.4°, 24.3°, 24.7°, 25.8°, 35.7° of the sample synthesized for different time to that of the well-crystallized sample for 24 h.

**Table S2.** Chemical composition (wt.%) of the $Pt_{0.6}$@ZSM-22-H and ZSM-22-H determined by XRF.

| Sample | $SiO_2$ | $Al_2O_3$ | $K_2O$ | $Na_2O$ | Cl | $PtO_2$ |
|---|---|---|---|---|---|---|
| $Pt_{0.6}$@ZSM-22-H | 98.54 | 0.15 | 0.51 | 0.09 | 0.01 | 0.71 |
| ZSM-22-H | 99.22 | 0.16 | 0.52 | 0.08 | 0.01 | - |

**Table S3.** EXAFS data fitting results of Pt of $Pt_{0.6}$@ZSM-22-H and $Pt_{0.6}$/ZSM-22-H.

| Sample | Path | CN | R(Å) | $\sigma^2$(Å$^2$) | $\Delta E_0$(eV) | R factor |
|---|---|---|---|---|---|---|
| Pt foil | Pt-Pt | 12 | 2.765±0.002 | 0.0051 | 8.2 | 0.0051 |
| $PtO_2$ | Pt-O | 6.0 | 2.023±0.004 | 0.0025 | 1.9 | 0.0046 |
| | Pt-Pt | 8.0 | 3.099±0.005 | 0.0028 | 9.1 | |
| | Pt-O | 6.0 | 3.657±0.012 | 0.0025 | 10.7 | |
| $Pt_{0.6}$@ZSM-22-H | Pt-O | 1.3±0.5 | 1.907±0.012 | 0.0077 | 9.8 | 0.0062 |
| | Pt-Pt | 4.0±0.5 | 2.754±0.005 | 0.0127 | 9.5 | |
| $Pt_{0.6}$/ZSM-22-H | Pt-O | 2.5±0.3 | 1.877±0.016 | 0.0062 | -8.4 | 0.0100 |
| | Pt-Pt | 3.0±0.3 | 2.679±0.013 | 0.0058 | -2.4 | |

CN, coordination number; R, the distance between absorber and backscatter atoms; $\sigma^2$, the Debye Waller factor value; $\Delta E_0$, inner potential correction to account for the difference in the inner potential between the sample and the reference compound; *R* factor indicates the goodness of the fit.

**Table S4.** Comparison of catalytic performances of various Pt-based and zeolite-based catalysts for the conversion of furfural (FFL) to furfuryl alcohol (FOL) in the liquid phase.

| Entry | Catalysts | Metal loading (wt.%) | T (°C) | $H_2$ (MPa) | Solvent | Conversion (%) | FOL Selectivity (%) | Ref. |
|---|---|---|---|---|---|---|---|---|
| 1 | Pt(5 wt.%)/$Al_2O_3$ | 4.7 | 180 | 2.0 | isopropanol | 91.0 | 89.1 | 1 |
| 2 | Pt/γ-$Al_2O_3$ | 1.9 | 80 | 0.1 | methanol | 80 | 99 | 2 |
| 3 | Pd@Na-ZSM-5 | 0.65 | 175 | 1.0 | isopropanol | - | 90.2 | 3 |
| 4 | 3% Pt/AC | 3.0 | 150 | 5.0 | cyclopentyl methyl ether | - | 29 | 4 |
| 5 | 3% Pt/AC | 3.0 | 200 | 3.0 | isopropanol | 93 | 51 | 4 |
| 6 | $Pt_3Fe/CeO_2$ | 2.0 | 100 | 2.0 | isopropanol | 99.8 | >99 | 5 |
| 7 | $Pt_1Sn_{0.3}$@HMSNs | 3.4 | 100 | 1.0 | isopropanol | 99.7 | 97.8 | 6 |
| 8 | Na-Cu@TS-1 | 2.05 | 110 | 1.0 | isopropanol | 93.0 | 98.1 | 7 |
| 9 | Pt/HT | 2.86 | 30 | 1.5 | water | 99.9 | >99 | 8 |
| 10 | Pt/MgO$Al_2O_3$ | 2.77 | 30 | 1.5 | water | 84.9 | ＞99 | 8 |
| 11 | Pt/MgO | 2.83 | 30 | 1.5 | water | 98.9 | ＞99 | 8 |
| 12 | Pt/$Al_2O_3$ | 2.84 | 30 | 1.5 | water | 52.9 | 88.6 | 8 |
| 13 | Pt/BN-U10-12 | 1.32 | 80 | 1.0 | isopropanol | 94.2 | 96.3 | 9 |
| 14 | Pt/$CeO_2$-270 | 2.96 | 80 | 1.0 | isopropanol | 100 | 97.3 | 10 |
| 15 | $Pt_{0.6}$@ZSM-22-H | 0.62 | 180 | 4.0 | isopropanol | 99.5 | 97.6 | This work |

**Table S5.** The absorption band assignment of IR spectrum of liquid-phase furfural, gas-phase furfural and adsorbed furfural.

| Furfural state | | Adsorption configuration | Peak wavenumber ($cm^{-1}$) | Assignment |
|---|---|---|---|---|
| Unadsorbed | Liquid[11, 12] | - | 1690/1675 | υ(C=O) |
| | | | 1565/1476/1466/1393 | Ring breath |
| | | | 1565/1473/1466 | υ(C=C) |
| | Gas[13-15] | - | 1720 | υ(C=O) |
| | | | 1578/1474 | Ring breath/υ(C=C) |
| | Physisorption[15] | - | 1694 | υ(C=O) |
| Adsorbed | Chemisorption [a] | $\eta_1$(O) | 1625-1685 | υ(C=O) |
| | | $\eta_2$(C, O) | 1460 | υ(C=O) |
| | | $\eta_1$(O) and $\eta_2$(C, O) | 1570/1473/1466/1396 | Ring breath |
| | | | 1570/1473/1466 | υ(C=C) |

[a] The chemical adsorption of furfural in this work; the adsorption of furan ring was not observed.

**Reference**


1. S. Bhogeswararao and D. Srinivas, *J. Catal.*, 2015, **327**, 65-77.
2. M. J. Taylor, L. J. Durndell, M. A. Isaacs, C. M. A. Parlett, K. Wilson, A. F. Lee and G. Kyriakou, *Appl. Catal., B*, 2016, **180**, 580-585.
3. Y. Chai, S. Liu, Z. Zhao, J. Gong, W. Dai, G. Wu, N. Guan and L. Li, *ACS Catal.*, 2018, **8**, 8578-8589.
4. Y. Wang, P. Prinsen, K. S. Triantafyllidis, S. A. Karakoulia, P. N. Trikalitis, A. Yepez, C. Len and R. Luque, *ACS Sustain. Chem. Eng.*, 2018, **6**, 9831-9844.
5. X. Gao, S. Tian, Y. Jin, X. Wan, C. Zhou, R. Chen, Y. Dai and Y. Yang, *ACS Sustain. Chem. Eng.*, 2020, **8**, 12722-12730.
6. T. Xiao, P. Yan, K. Li, C. Yang, H. Yu, J. Wang, H. Yin and S. Zhou, *Ind. Eng. Chem. Res.*, 2021, **60**, 6078-6088.
7. P. Cao, L. Lin, H. Qi, R. Chen, Z. Wu, N. Li, T. Zhang and W. Luo, *ACS Catal.*, 2021, **11**, 10246-10256.
8. G. Gao, J. Remon, Z. Jiang, L. Yao and C. Hu, *Appl. Catal., B*, 2022, **309**, 121260.
9. D. Yan, J. Li, M. Zahid, J. Li and Y. Zhu, *Applied Surface Science*, 2023, **609**, 155308.
10. Q. Yang, D. Gao, C. Li, S. Wang, X. Hu, G. Zheng and G. Chen, *Appl. Catal., B*, 2023, **328**, 122458.
11. G. Allen and H. J. Bernstein, *Can. J. Chem.-Rev. Can. Chim.*, 1955, **33**, 1055-1061.
12. H. Ashish and P. Ramasami, *Mol. Phys.*, 2008, **106**, 175-185.
13. S. Sitthisa, T. Sooknoi, Y. Ma, P. B. Balbuena and D. E. Resasco, *J. Catal.*, 2011, **277**, 1-13.
14. X. Meng, Y. Yang, L. Chen, M. Xu, X. Zhang and M. Wei, *ACS Catal.*, 2019, **9**, 4226-4235.
15. Q. Wang, J. Feng, L. Zheng, B. Wang, R. Bi, Y. He, H. Liu and D. Li, *ACS Catal.*, 2020, **10**, 1353-1365.